



HAL
open science

Experimental superheating and cavitation of water and solutions at spinodal-like negative pressures

Lionel Mercury, Kirill Shmulovich

► **To cite this version:**

Lionel Mercury, Kirill Shmulovich. Experimental superheating and cavitation of water and solutions at spinodal-like negative pressures. *Transport and Reactivity of Solutions in Confined Hydrosystems*, Springer, pp.159-171, 2014, Series: NATO Science for Peace and Security Series C: Environmental Security, 978-94-007-7533-6. 10.1007/978-94-007-7534-3_14 . insu-00906681

HAL Id: insu-00906681

<https://insu.hal.science/insu-00906681>

Submitted on 20 Nov 2013

HAL is a multi-disciplinary open access archive for the deposit and dissemination of scientific research documents, whether they are published or not. The documents may come from teaching and research institutions in France or abroad, or from public or private research centers.

L'archive ouverte pluridisciplinaire **HAL**, est destinée au dépôt et à la diffusion de documents scientifiques de niveau recherche, publiés ou non, émanant des établissements d'enseignement et de recherche français ou étrangers, des laboratoires publics ou privés.

Abstract. The superheated liquids are metastable with respect to their vapour, what means they can exist under arid conditions whatever the temperature: capillary liquid extracted from arid soils (desert shrubs, Mars sub-surface, ...), solutions in the deep Earth crust, or water involved in rapid disequilibrium events (terrestrial or submarine geysers). The superheating state changes the solvent properties of liquids, and so modifies phase transitions (solid-liquid, liquid-vapor) P-T-X conditions. The synthetic fluid inclusion (SFI) enables to fabricate micro-volumes of hand-made liquid dispersed inside quartz, which readily superheat. Volumes of SFI are intermediate between macro-systems, in which superheating is restricted to around -30-35 MPa with very short lifetime, and nanosystems, wherein confinement effects predominate and in which the host size is similar to the one of the critical nucleus of vapour phase (huge nucleation barrier). This volume-to-metastability relationship is still to be defined quantitatively, and we are targeting to combine thermometric classical measurements with spectrometric characterizations, enabling to establish the threshold between micro- and nano-systems precisely. Meanwhile, the experiments performed so far illustrate the diversity of contexts and situations that could be impacted by superheating issues.

1. INTRODUCTION

Liquid water presents a remarkable ability to stay liquid against evaporative demand by becoming superheated with respect to water vapor. Water can be readily superheated by increasing the temperature higher than 100°C at constant 1 atm pressure, or by decreasing its internal pressure, it becomes superheated even at low temperature (Fig. 1a). Meanwhile, the driving force is toward evaporation and so the liquid is prone to nucleate bubbles at any time, except if some reasons, notably the trapping in a host solid, make the nucleation probability to decrease and the lifetime to lengthen (Fig 1b). It is why superheating is a feature closely interwoven with capillarity and confinement, in which cases the closeness of the solid walls make the infilling liquid to behave differently than the bulk.

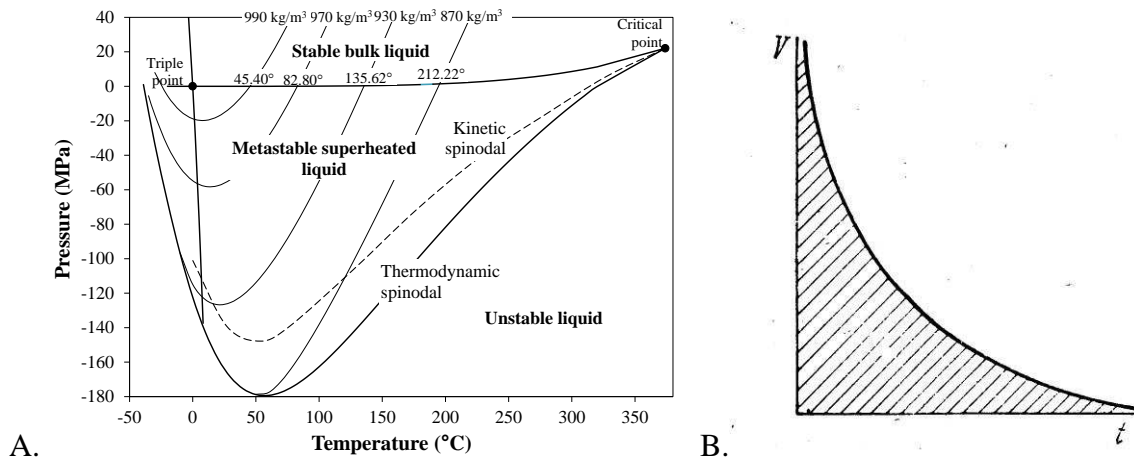


Fig. 1. A. Phase diagram of pure water in P-T space, calculated with the IAPWS-95 equation of state [1]. Kinetic spinodal is drawn after [2]. B. Qualitative relationship between space volume allowed to liquid and lifetime of its superheating (potential) state (after [3]).

As a consequence, the conditions of occurrence and the features of superheated water are relevant to understand the dynamics of liquid water in arid (deserts) and hyper-arid (Mars surface) settings, and its possible volume and influence as a function of the environment. Experimentally, the most efficient way to produce superheated liquid is to carry out an isochoric cooling on a liquid trapped in a strictly closed container with rigid walls. With water, as the isochores are very steep (around 20 bars per degree) and the saturation curve is very flat, a slight cooling below liquid-vapor equilibrium puts the occluded liquid under significant superheating degree, even down to negative pressures (Fig. 1a). Negative pressure or tension, is allowed for condensed matter that thus undergo internal stretching or tensile stress without losing the cohesion of its structure (e.g., [4]).

Capillary water, common in non-saturated soils, has got superheated properties without its limited lifetime because the capillary channel/pore has the size of the nucleating bubble, meaning that the boiling restoring equilibrium cannot start.

In this sense, capillary water is a superheated water “de-metastabilized” or “re-stabilized” by geometrical constraints defined by the so-called Young-Laplace equation. At the liquid-air interfaces, capillary water is at equilibrium with dryer atmosphere than the bulk (Kelvin law), which is the driving force to “capillarization”. Actually, lower vapor pressure than the saturation value drives a liquid-vapor system to either evaporation or capillarity.

Water located in restricted volume (“confined water”) has also peculiar properties due to the additional thermodynamic term afforded by the surface fields from the close walls (disjoining pressure effect). In many respect, confined water has got similar properties than the capillary or superheated water. Interestingly, confinement experimentally exhibits metastable behaviors (e.g., [5-6]).

The present contribution reports experimental data obtained with synthetic fluid inclusions on the extreme tensile strengths (negative pressure) that pure water and aqueous solutions can attain and on the lifetime over which they can sustain them. It has also the ambition to enlist the possible consequences of superheating (and so capillarity, and/or confinement) in terms of macroscopic behaviors. Putting the liquid under extreme conditions of tension gives pathway to measure directly how the superheating properties, even moderate, may drive specific behavior in the corresponding natural settings.

2. EXPERIMENTAL SECTION

Synthetic Fluid Inclusions (SFI) are made in internally-heated pressure vessels (IHPV, or “gas bombs”). The hydrothermal syntheses were performed at 750 MPa in the 530-700°C range, during 8 to 13 days. For each run, the IHPV is loaded with 3 or 4 Pt-capsules filled with quartz (2x2x12 mm, with the longest dimension parallel to the quartz c-axis), the selected liquid (pure water or aqueous solutions at the chosen concentration) and amorphous silica. Sealed capsules were placed on a Ta or Mo holder wherein the temperature is controlled by two Pt-Pt 13% Rh thermocouples (certified to $\pm 1^\circ$), and pressure measured by manganin gauges after calibration at the mercury melting point. Once the required synthesis time elapsed, the power supply is turned off and temperature decreases to 100°C in one minute, while pressure is decreased by intensifier to 300 MPa. In a second step, the IHPV is allowed to cool down on its own to room temperature and is finally opened to recover the capsules and quartz samples the healing of which trapped the liquid.

The microthermometric procedure consists of progressive heating on a “Linkam” stage of one sample, in general containing initially the biphasic liquid+vapour assemblage (L+V).

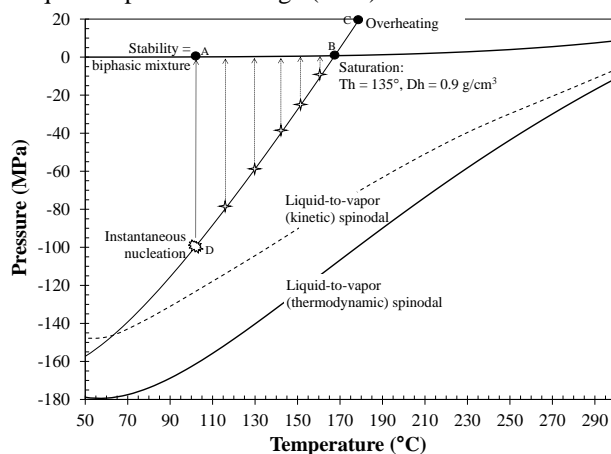


Fig. 2. Classic microthermometric path from the ambient conditions (see text). Nucleation can appear instantaneously (T_n commonly measured by inclusionists, sparky point) or after a delay (starry points) if the temperature is stopped before reaching the instantaneous T_n .

The first step corresponds to the displacement along the saturation line, with a progressive change of temperature, liquid density and bubble pressure (A to B path, Fig. 2). At a particular density, the trapped liquid invades the whole inclusion space: there is no more vapour and the inclusion is said to be homogenized (B point, Fig. 2). The temperature at which this filling appears is then the homogenization temperature, noted T_h . Just before T_h , vapour bubble is so small that it can move along the minor thermal gradients within the inclusion, which results in the appearance of a mobile shadow. Further heating drives the P-T conditions in the inclusion along the isochore inside the stable domain of liquid (B to C path, Fig. 2). Special care must be taken because overheating above T_h may lead to the decrepitation of the inclusion, especially at overheating greater than 30°C (but 10°C can be sufficient; see also [7]): this depends also on (at least) the shape of the inclusion, its thickness and the distance to neighboring inclusions. One decrepitation event can be detected when a further T_h measurement on the same inclusion increases by more than 1°C with respect to antecedent measurements. The second step is the progressive cooling of the sample, which follows the isochoric path as long as the

inclusion remains homogeneously filled with liquid (C to D path without nucleation at B, Fig. 2). The temperature of the bubble appearance is called the nucleation temperature (T_n) and is always located within the tensile domain: nucleation in fluid inclusions often disobeys the saturation conditions. The bubbling at T_n produces either one-two big bubbles or a large amount of intermediate-sized bubbles which explode violently.

3. SUPERHEATING LIMITS AND LIFETIME

3.1 Measurements and interpretation

The basic measurements are then of two types: first the ($T_h - T_n$) gap at which instantaneous nucleation occurs, and the time needed for a nucleation to occur for any temperature set between T_h and T_n (Fig. 3). The present dataset is reported in figure 3, and lists hundreds of inclusions measured in more than 40 samples. ($T_h - T_n$) gap are strongly liquid- and temperature-dependent, varying the most for CsCl electrolytic solutions at low T (scattering over 80°C) and denser pure water (scattering over 70°C). The smallest gaps are encountered with dilute NaOH solutions whatever the temperature, and for each type of solutions, the gap is narrowing with increasing temperature. This last feature fits well the expected behavior considering the narrowing of the saturation to spinodal gap with temperature (Fig. 1). A close discussion of the different trends is outside the scope of this paper, some aspects are developed elsewhere [8].

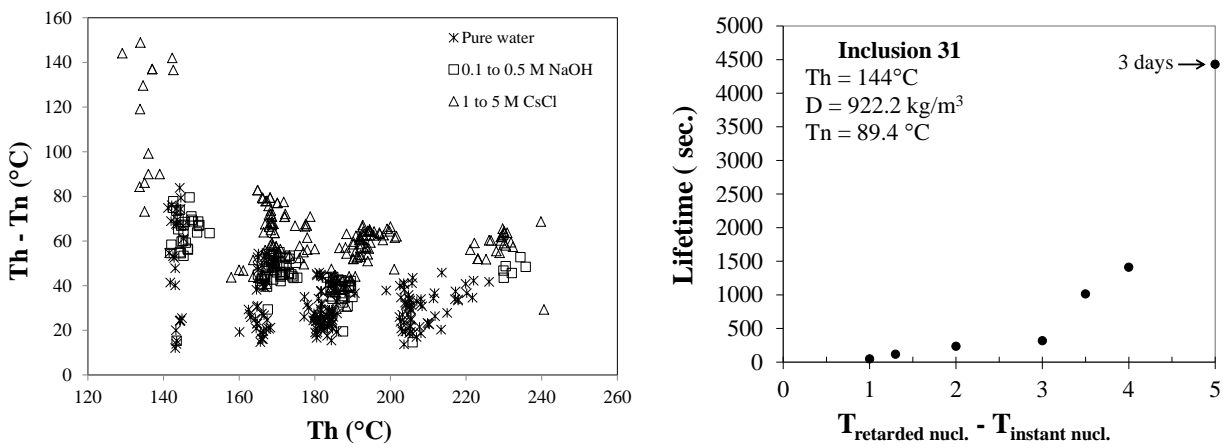


Fig. 3: Measurements classically performed on liquids trapped in SFI by microthermometry: temperature gap to observe instantaneous nucleation, and lifetime of superheated state.

The conversion of micro-thermometric measurements into internal pressure of superheated liquids requires using an equation of state (EoS). Basically, measuring T_h enables to define the density of the trapped liquid at homogenization (D_h). Assuming a perfectly isochoric cooling, the couple (T_n, D_h) can be readily turned into (T_n, P_n), with P_n stands for the internal pressure inside liquid just before nucleation (Fig. 4).

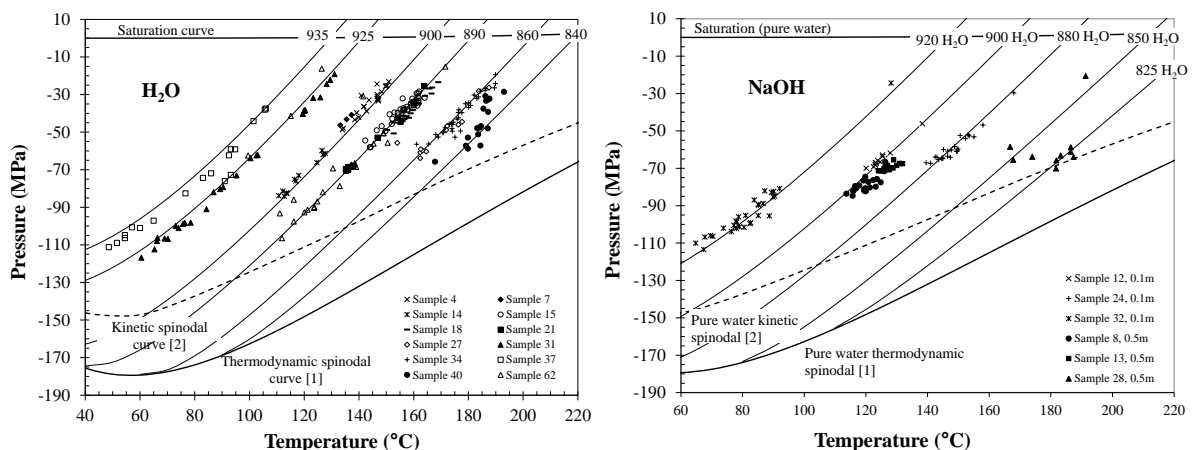
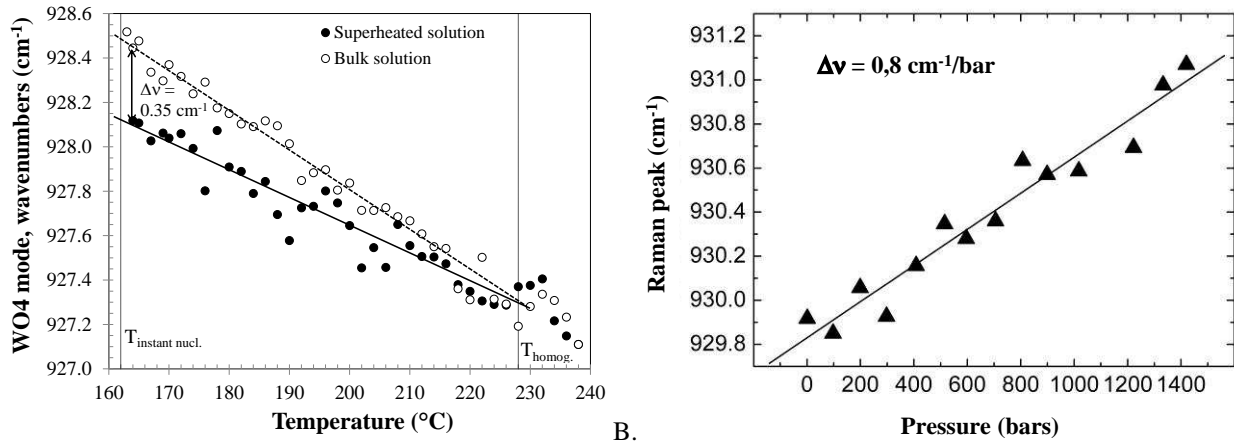


Fig. 4: P-T phase diagram, including the (T_h, T_n) measurements of different datasets turned into (P, T) data points (see text) using the IAPWS-95 equation of state for water [1].

Two questions are actually embedded in such procedure: i) applicability of EoS to superheating state, and ii) having the EoS characteristic of the measured solutions. About the first issue, pure water EoS can be readily used for dilute solutions, in which most of the molar content is made of water molecules (Fig. 4). However, studying the saline solutions require to extrapolate the available EoS, not always internally-consistent, toward the metastable state (e.g., [9]). As a consequence, interpretation are certainly correct in terms of global trends, but cannot be considered as

quantitatively precise for the time being. About the second issue, the general feeling is toward admitting the continuity of behavior from stability to metastability, meaning that superheated water is no more than a “particular” state of otherwise-bulk liquid (e.g. [10-13]), but, here again, some doubts still need to be lifted.

A current experiment tries to quantify the internal stress in fluid inclusions, by recording direct signals of the pressure change directly inside the inclusion, shunting any use of EoS. To do this, an aqueous solution of Na_2WO_4 has been trapped in inclusion, because the Raman peak of this anion is pressure-dependent. Running classic micro-thermometry path into a Raman spectrometer resulted in a continuous Raman shift that demonstrates an increasing tension inside the trapped solution. This experiment solved the challenge on the measurement itself (the shift is lower than the absolute precision of the spectrometer) and provided direct evidence on the internal tension of the occluded liquid: extrapolating the positive pressure behavior (Fig. 5B), the tension comes to -432 bars. However, this experiment has not fully answered the question, since these Raman measurements cannot be compared to EoS calculations, not existing for Na_2WO_4 . Complementary experiments are under way.



A. Spectroscopic pressure measured by the Raman shifts of the tungstate dissolved in tensile solutions trapped in SFI. B. Calibration at positive pressure.

3.2 Lifetime and cavitation

In terms of lifetime, the measurements have been fitted by the Classical Nucleation Theory (CNT) which considers the work of creating LV surface compared to the work brought about by the higher stability of the vapor embryo. Interestingly, the CNT equation for homogeneous nucleation (the source of work in the system is the thermal fluctuations) does not fit the data, but that for the heterogeneous nucleation on a hydrophobic (and pure quartz is) surface does (Fig. 6).

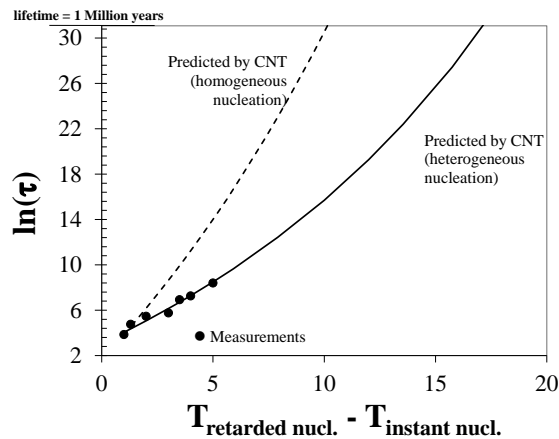


Fig. 6: Lifetime of superheated pure water SFI in quartz ($50 \times 20 \mu\text{m}$; [14]), plotted against the distance to temperature of instantaneous nucleation (Fig. 2). The heterogeneous CNT equation is from [15], compared to the usual homogeneous CNT one (e.g., [16]).

These are preliminary results since the data are only acquired over 3 days for restricted distance to instantaneous nucleation ($\Delta T_{\text{max}} = 6^\circ\text{C}$). Interestingly, the extrapolation of the fitted trend indicates that a very long metastable lifetime is possible even for significant superheating state ($\Delta T \approx 18^\circ$, possibly corresponding to a tension down to -500 bars). The present target is to confirm the validity of the heterogeneous CNT equation toward extrapolation, by performing longer experiments increasing the range of distance to equilibrium.

One interesting feature should be additionally addressed: the role of the host volume to stabilize the superheating as evoked in figure 1. This question is beyond a simple academic interest and corresponds to understand the size threshold below which the confinement effect would suppress the nucleation event, allowing to safely produce highly superheated liquid.

A first clue comes from an open question in the physics of metastability [17]: among the different techniques available to produce superheating, only the SFI enables to reach high level of metastability (Fig. 7A). A key difference between SFI and all other technique is the way the liquid volume occupy the experimental cell. In case of dynamic/capillary techniques there is only one experimental water volume, so that the first nucleation event makes all the volume to boil. In case of inclusions samples, liquid is dispersed as numerous micrometric cavities in the same solid fragment, and the vapour nucleates at P,T conditions peculiar to each inclusion. That means the geometrical confinement, even over hundreds of micrometers (which make a pretty large volume), should help in pushing the superheating state at larger value in inclusions than in the other experimental cells without walls.

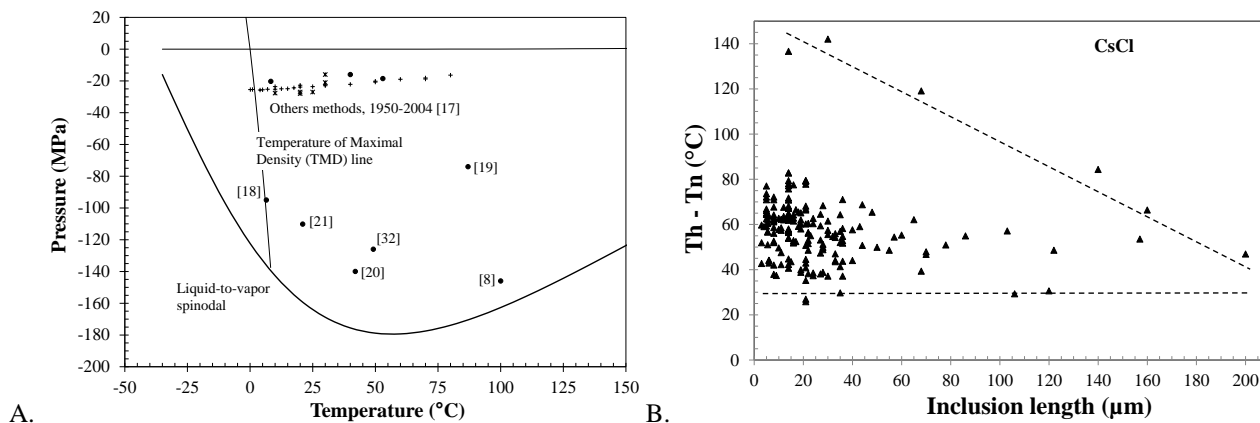


Fig. 7: A. Extreme tensile strength obtained with different static and dynamic methods [17-21]. Black dots are Berthelot tubes and SFI. B. Relationship in CsCl-filled samples (1 and 5m CsCl) between $(Th - T_n)$ and the volume of the inclusions (1D simplification) (dotted lines are only guides for eyes).

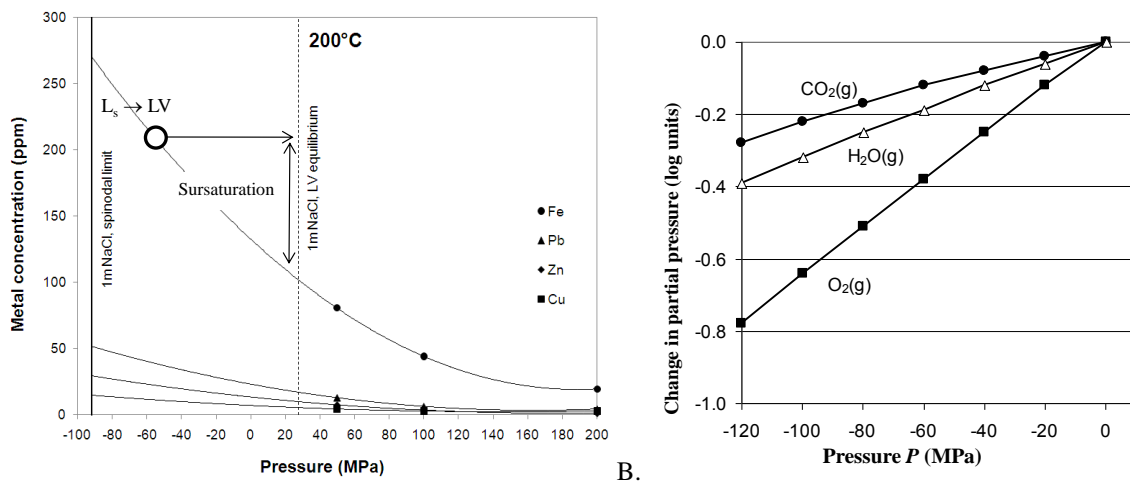
A second clue is afforded by the common relationship between the $(Th - T_n)$ metastability gap and the host volume (e.g., [8], see their figure 8a,b). However, as apparent in figure 7B, this relationship is common but has exceptions or limits (see also figure 8b in [8]), demonstrating that other factors are embedded in this size factor, for instance the internal shape of the inclusions that reveals its degree of equilibrium (“negative quartz shape”) [8]. Even Th itself can vary (over 1-3°C) with the size of inclusion due to surface tension effects [22]. In another direction, the size of the inclusion and the internal faceting of the space void, partly control the properties of the SFI, notably the modes of their non-elastic deformation (stretching, leakage, decrepitation) [7].

Here again, complementary experiments are needed to decipher how the size of inclusions combine with other critical factors to control the behavior of inclusions, notably the extent of metastability and the deformability.

4. EXPECTED BEHAVIOUR OF SUPERHEATED (CAPILLARY & CONFINED) WATER

4.1 Geochemistry of phase transitions

Capillary liquids have the same properties of superheated water, and most probably confined water as well. Superheated water is known to be a very good solvent for organics compounds as pesticides, making it the “ultimate green solvent for separation science” (e.g., [23-24]). This experimental observation can be easily illustrated extrapolating the solubility line of different metals sulfides in aqueous solution beyond the saturation LV line, down to the spinodal (Fig. 8A). Additionally, the diagram shows that the cavitation which restores the equilibrium changes the saturation conditions and contributes to precipitate the excess dissolved mass. Interestingly, a recent study showed the ice nucleation just following the bubble cavitation in superheated water [25].



A. Solubility line, empirically extrapolated at negative pressures, illustrating the solvent effect of superheated (capillary/confined) liquid (after [8]). B. Gases solubility as a function of the internal tension in superheated/capillary water (modified from [26]).

In the second part of the figure, it appears that the gases are more soluble in superheated/capillary water than in bulk water. Actually, this in-gassing effect could be of significant importance to understand the global carbon cycle: the immobile water trapped under tension in the capillary clusters of all the arid and semi-arid soils of Earth are pumping in more atmospheric CO₂ than expected without considering the capillary role on dissolution. These findings are mitigated by the small volume of capillary water at dry conditions that limits the total mass that can be actually stored in soils.

4.2 Geochemistry and geomechanics

The liquid under tension when trapped in solids exerts traction on the host solid, and so contributes to the geomechanical balance at the pore scale [27]. Drying experiments performed in micrometric round pore showed that a first precipitation of cubic salt allowed the arising of capillary bridge at the salt-pore contacts that generated a deformation of the host (Fig. 9A).

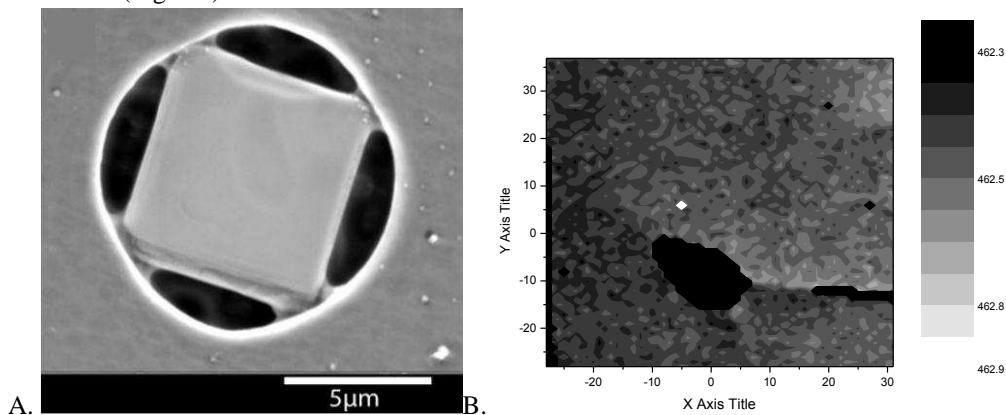


Fig. 9: A. Cubic NaCl precipitation in round pore (radius = 5 μm), secondary precipitation of concave-curved NaCl at the prior salt-pore contacts, and resulting deformation. B. Raman shift inside the quartz matrix around an inclusion filled with 5m CsCl, and put at (Th-Tn) = 90°C (unpublished results; Collab. CEMTHI, P. Simon).

Another experiment is presently running, searching to record the constraints implied in the surrounding solid by the tension inside a highly superheated electrolytic aqueous solution (Fig. 9B). Interestingly, part of the surrounding quartz is under slight tension (darkest part, to the left of the inclusion), while another part is under compression (dark/light grey, to the right of the inclusion). These two compartments are easily distinguished by two lines making a 120° angle between, classic in crystalline quartz. The current interpretation is that the in-inclusion tension pulls up the right compartment that moves as a wedge and so is put under overpressure, while the other rigid compartment does not move and undergo the tensile elastic deformation. This first experiment demonstrates the complexity of the stress field all around an inclusion, active as long as the liquid tension is effective, and evidences the compensation effects due to the heterogeneity on the matrix itself.

4.3 Explosivity

A superheated liquid is metastable with respect to its vapour and then able to nucleate at any moment (Fig. 10A). During the 18th century, Rev. Dayton already reported on the easiness to superheat a liquid and the associated explosive

danger [28]. Nowadays, this is a well-known class of industrial spills accidents, connected to the Boiling Liquid Expanding Vapour Explosion (BLEVE) type (for instance, [29]). As thermodynamically demonstrated [9], the superheating state of the mother liquid does not increase so much the energy release at the LV phase transition, but dramatically increases the rate of this transition. The power of one explosion is the product of the energy release by the time of release, it comes to the superheating boiling can be qualified as explosive because it is a rapid-phase transition whose rapidity is depending on the superheating “level” [29].

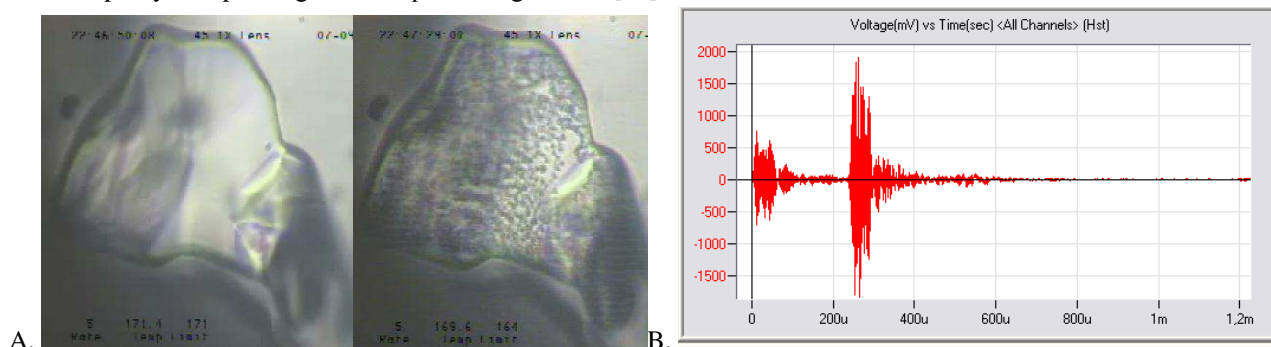


Fig. 10: A. Intense and brutal boiling in 5m NaCl: Th = 221°C; Th-Tn = 51°C (also at <http://www.iem.ac.ru/staff/kiril>). B. Soundwave accompanying the trapped liquid cavitation recorded by an acoustic emission sensor (Euro Physical Acoustics).

The cavitation event produces a sound wave that can be recorded to characterize the intensity of the prior metastability and estimate the mass that cavitates (Fig. 10B). Additionally, several sensors can be used to detect the exact location of cavitation which is not so valuable when working with transparent material like quartz SFI, but could become interesting if using this system to record cavitation event in heterogeneous porous systems.

Interestingly, the boiling of large bubbles in porous soils was evoked as a potentially important factor to the transport in porous media (e.g., [30-31]). Actually, this boiling occurs in water immobilized against gravity due to the capillary forces. The boiling breaking out this capillary suction makes the water body able to flow again according to the gravitational field. This de-metastabilization event can also be expected to move an initially continuously water body into a sum of dispersed flowing/not-flowing water clusters, shaping a discontinuous water content in soils.

CONCLUSION

Superheated water is a special state which appears for different reasons (decreasing vapor pressure, increasing temperature) and can be useful for different purposes. First, the properties of superheated water are of interest for those situations during which this special metastable state arises. Second, these properties also fit the capillary properties, because capillarity is no more than a superheated state without metastability. However, an open question is the role the superheating plays in the confinement of liquid in geometrical restricted pore spaces. But again, the superheated properties could fit well with the confinement behavior.

On another point of view, this study outlines the shortage of knowledge about the consequences in natural settings to contain liquid water with superheated properties (whatever its actual form: confined, capillary, or strictly superheated). In particular, the phase transitions (gas/solid-solution interactions, liquid-vapor explosive boiling) are drastically changed that could impact significantly our understanding of the mass transfer in the corresponding pore networks. All the results showed here need to be extended and generalized, and relativized to the surface area of the liquid-solid interface, and also to the volume of liquid involved and available for the reaction. A completely overlooked aspect is the retention/flow duality and more generally the consequences of the superheating on the transport functions of the infilling pores liquid.

ACKNOWLEDGMENTS

This work has received support from the French Agency for Research (Agence Nationale de la Recherche, ANR) through the grant CONGE BLAN-61001 and ANR-10-LABX-100-01.

REFERENCES

- [1] Wagner W. and Pruss A. (2002) The IAPWS Formulation 1995 for the Thermodynamic Properties of Ordinary Water Substance for General and Scientific Use. *J. Phys. Chem. Ref. Data* 31, 2, 387-535.
- [2] Kiselev S.B. and Ely J.F. (2001) Curvature effect on the physical boundary of metastable states in liquids. *Physica A* 299, 357-370.

- [3] Skripov V.P., Sinitsyn E.N., Pavlov P.A., Ermakov G.V., Muratov G.N., Bulanov N.V., and Baidakov V.G. (1988) Thermophysical properties of liquids in the metastable (superheated) state, Gordon and Breach Science Publishers.
- [4] Imre A., Martinas K., and Rebelo L.P.N. (1998) Thermodynamics of negative pressures in liquids *J. Non-Equilib. Thermodyn.* 23, 4, 351-375.
- [5] Restagno F., Bocquet L., and Biben T. (2000) Metastability and nucleation in capillary condensation. *Phys. Rev. Lett.* 84(11), 2433-2436.
- [6] Morishige K. and Yasunaga H. (2006) Tensile effect on a confined phase. *J. Phys. Chem. B* 110, 3864-3866.
- [7] Bodnar R.J., Binns P.R., and Hall D.L. (1989) Synthetic fluid inclusions. VI. Quantitative evaluation of the decrepitation behavior of fluid inclusions in quartz at one atmosphere confining pressure. *J. Metamorphic geol.* 7, 229-242.
- [8] Shmulovich K.I., Mercury L., Thiéry R., Ramboz C. et El Mekki M. (2009) Experimental superheating of water and aqueous solutions. *Geochim. Cosmochim. Acta* 73(9), 2457-2470.
- [9] Thiéry R. and Mercury L. (2009) Explosive properties of water in volcanic and hydrothermal systems. *J. Geophys. Res.* 114, B05205, doi:10.1029/2008JB005742..
- [10] Skripov V.P. (1992) Metastable states. *J. Non-Equilib. Thermodyn.* 17, 193-236.
- [11] Mercury L., Azaroual M., Zeyen H., and Tardy Y. (2003) Thermodynamic properties of solutions in metastable systems under negative or positive pressures. *Geochim. Cosmochim. Acta* 67, 1769-1785.
- [12] Mercury L., Jamme F. et Dumas P. (2012) Infrared imaging of bulk water and water-solid interfaces under stable and metastable conditions. *Phys. Chem. Chem. Phys.* 14, 2864-2874
- [13] Davitt K., Rolley E., Caupin F., Arvengas A., and Balibar S (2010) *J. Chem. Phys.* 133, art. 174507.
- [14] El Mekki M., Ramboz C., Perdereau L., Shmulovich K.I., and Mercury L. (2009) In "Metastable systems under pressure". NATO Science for Peace and Security Series A, Chemistry and Biology. Edited by S.J. Rzoska, A. Drozd Rzoska et V. Mazur. Springer Verlag, p.279-292.
- [15] Blander M. and Katz J.L. (1975) Bubble nucleation in liquids; *AIChE J.* 21 (5), 833-848.
- [16] Debenedetti, P.G., 1996. Metastable liquids. Concepts and principles. Princeton University Press.
- [17] Caupin F. and Herbert E. (2006) Cavitation in water: a review. *C.R. Phys.* 6, 1000-1017.
- [18] Roedder E. (1967) Metastable superheated ice in liquid-water inclusions under high negative pressure. *Science* 155, 1413-1417.
- [19] Green J.L., Durben D.J., Wolf G.H. and Angell C.A. (1990) Water and solutions at negative pressure: Raman spectroscopic study to -80 Megapascals. *Science* 249, 649-652.
- [20] Zheng Q., Durben D.J., Wolf G.H. and Angell C.A. (1991) Liquids at large negative pressures: water at the homogeneous nucleation limit. *Science* 254, 829-832.
- [21] Alvarenga A.D., Grimsditch M., and Bodnar R.J. (1993) Elastic properties of water under negative pressures. *J. Chem. Phys.* 98, 11, 8392-8396.
- [22] Fall A., Rimsditch J.D., and Bodnar R.J. (2009) The effect of fluid inclusion size on determination of homogenization temperature and density of liquid-rich aqueous inclusions. *Am. Mineral.* 94, 1569-1579.
- [23] Smith R.M. (2006) Superheated water: the ultimate green solvent for separation science. *Anal. Bioanal. Chem.* 385, 419-421.
- [24] Chienthavorn O. And Su-in P. (2006) Modified superheated water extraction of pesticides from spiked sediment and soil. *Anal. Bioanal. Chem.* 385, 83-89.
- [25] Barrow M.S., Williams P.R., Chan H.-H., Dore J.C., and Bellissent-Funel M.-C. (2012) *Phys. Chem. Chem. Phys.* 14, 13255-13261.
- [26] Mercury L., Pinti D. L., and Zeyen H. (2004) The effect of the negative pressure of capillary water on atmospheric noble gas solubility in groundwater and palaeotemperature reconstruction. *Earth & Planetary Sci. Lett.* 223, 147-161.
- [27] Bouzid M., Mercury L., Lassin A., Matray J.-M. et Azaroual M. (2011) . In-pore tensile stress by drying-induced capillary bridges inside porous materials. *J. Colloid Interf. Sci.* 355, 494-502.
- [28] Dayton J. (1739) An experience to prove, that water, when agitated by fire, is infinitely more elastic than air in the same circumstances. *Phil. Trans.* 41(1), 162-166.
- [29] Reid R.C. (1976) Superheated liquids. *Amer. Sci.* 64, 146-156.
- [30] McManus K.J. and Davis R.O. (1997) Dilation-induced pore fluid cavitation in sands. *Géotechnique* 47(1), 173-177.
- [31] Or D. and Tuller M. (2002) Cavitation during desaturation of porous media under tension. *Water Resour. Res.* 38(5), 1061, doi: 10.1029/2001WR000282.
- [32] El Mekki Azouzi M., Ramboz C., Lenain J.F., and Caupin F. (2012) A coherent picture of water at extreme negative pressure. *Nature Physics*, doi: 10.1038/NPHYS2475.